Progress In Electromagnetics Research Letters, Vol. 108, 15–23, 2023

Research on Multi-Band Absorbers Based on Electromagnetic Metamaterials

Fugui Liu[1], Bin Xu[1], Xiaonan Li[2, *], and Guoqiang Liu[2]

Abstract—The rapid development of telecommunication systems has promoted the research of electromagnetic metamaterial absorbers. Based on the equivalent circuit theory, this paper proposes and designs a broadband absorption absorber based on electromagnetic metamaterials, which adopts a sandwich structure with an overall absorber thickness of 3.234 mm. The results show that the absorber has an absorption rate of more than 90% in the X-, Ku-, and K-bands (8.06 GHz–18.46 GHz) for the incident angle varying in the range of 0–50°. The absorption rate is higher than 90% for TE and TM mode electromagnetic waves and electromagnetic waves with polarization angle in the range of 0–50°. The absorber still has good absorption characteristics. The study shows that the absorber has small size, thin thickness, and broad angle broadband absorption characteristics.

1. INTRODUCTION

Electromagnetic metamaterials generally refer to artificial periodic structures or composites that possess extraordinary physical properties that natural materials do not [1]. The size of the structure is generally much smaller than the working wavelength. The extraordinary physical properties of electromagnetic metamaterials are usually manifested as a negative refractive indexand negative dielectric constant [2]. With scholars' in-depth research, electromagnetic metamaterials are usually applied in polarisation conversion, absorbers, and other fields [3–7]. Due to the rapid development of telecommunication systems, the research of electromagnetic metamaterial oscilloscopes has been promoted. In the design of such absorbers, two main factors should be considered: the size of the cell structure and the bandwidth of the absorption band.

The cell structure size can be reduced by increasing the size of the equivalent component values in the equivalent circuit on the surface of the resonant metal layer, e.g., the capacitance value. Among other things, the spacing between the metals in the resonant metal layer and the air gap between the resonant metal layer and the grounded metal backing provides a certain level of capacitance [8]. Using this technique, Bui et al. introduced a serpentine structure to miniaturise the cell structure and enable operation in the 400 MHz band [9]. Khuyen et al. proposed an ultra-thin absorber based on aggregate capacitance and vertical interconnection between the resonant metal layer and the metal backplane, covering the VHF band (centred on 102 MHz) [10]. In [11] by Zuo et al., for the UHF band (910 MHz) of the radio frequency identification system (RFID), a suction oscillator was designed, which used a structure with a linear zigzag shape and a combination of aggregate elements and air gap. The absorber designed in the current literature suffers from a complex structure, large thickness, which is not conducive to processing and fabrication, and a narrow absorption bandwidth.

To increase the absorption bandwidth of absorbers, scholars have introduced resonant units of electromagnetic metamaterial absorbers of different sizes, angles, and shapes as one way of designing

Received 2 October 2022, Accepted 4 November 2022, Scheduled 2 December 2022
* Corresponding author: Xiaonan Li (lxn@mail.iee.ac.cn).
[1] State Key Laboratory of Reliability and Intelligence of Electrical Equipment, Hebei University of Technology, Tianjin 300130, China. [2] Institute of Electrical Engineering, Chinese Academy of Sciences, Beijing 430074, China.

broadband absorbers [12, 13]. In another approach, researchers use complex geometric patterns to generate multiple resonances in a metallic resonant layer structure. The absorber is used to design three-band absorbing electromagnetic metamaterials in combination with a ring-shaped four-arrow metal resonant layer structure [14]. Different shapes of nested rings, such as three nested circular rings [15] and three square rings [16, 17], have also been proposed in the literature for the design of three-band electromagnetic metamaterial absorbers. As mentioned above, by adjusting the resonant layer's structure, the absorber's absorption bandwidth can be increased, and broadband absorption can be achieved.

The resonant metal layer of the broadband absorber designed in this paper achieves broadband absorption in the X-, Ku-, and K-bands by using a metal square ring and four rectangular metal structures. The absorber is not only small in size and thin in thickness but also polarisation-insensitive with wide-angle broadband absorption, making it a practical solution.

2. DESIGN AND THEORY

In this paper, the designed absorber is a sandwich structure with a metal resonant layer on the top, an FR-4 dielectric layer in the middle, and a metal backplane at the bottom. The equivalent circuit model of the designed electromagnetic metamaterial absorber is shown in Figure 1.

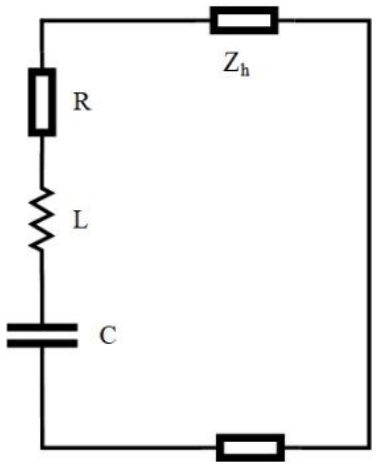

Figure 1. Equivalent circuit model of electromagnetic metamaterial absorber.

In this way, the impedance characteristics of the designed absorber are analysed. According to the impedance matching theory, the absorber's effective impedance can be adjusted to match the free space's impedance. Thus, the electromagnetic wave enters the absorber and is not reflected. The calculation of the specific equivalent impedance [15, 18] can be based on Equation (1)

$$Z(\omega) = \sqrt{\frac{\mu(\omega)}{\varepsilon(\omega)}} = \sqrt{\frac{[1 + S_{11}(\omega)^2]^2 - S_{11}(\omega)^2}{[1 - S_{11}(\omega)^2]^2 - S_{11}(\omega)^2}} \tag{1}$$

The law of energy conservation shows that the absorbed electromagnetic wave is electromagnetic wave energy minus the transmitted electromagnetic wave energy. That is, the absorption rate can be expressed as Equation (2).

$$A(\omega) = 1 - R(\omega) - T(\omega) \tag{2}$$

In Equation (2), $R(\omega)$ and $T(\omega)$ are the reflectance and transmittance shown in Equations (3) and (4), respectively.

$$R(\omega) = |S_{11}|^2 \tag{3}$$

$$T(\omega) = |S_{21}|^2 \tag{4}$$

When the reflectivity and transmittance of electromagnetic waves are both approximately 0, the absorption rate of the electromagnetic metamaterial absorber is approximately 1, which achieves the effect of perfect wave absorption.

3. STRUCTURAL DESIGN AND SIMULATION OPTIMIZATION

Assuming that the electromagnetic wave is incident from port 1 to the surface of the absorber, according to the propagation characteristics of the electromagnetic wave, part of the electromagnetic wave will be reflected from the surface of the absorber back to port 1. Another part of the electromagnetic wave will be transmitted through the absorber to port 2, and the propagation characteristics of the electromagnetic wave in the absorber are shown in Figure 2(a).

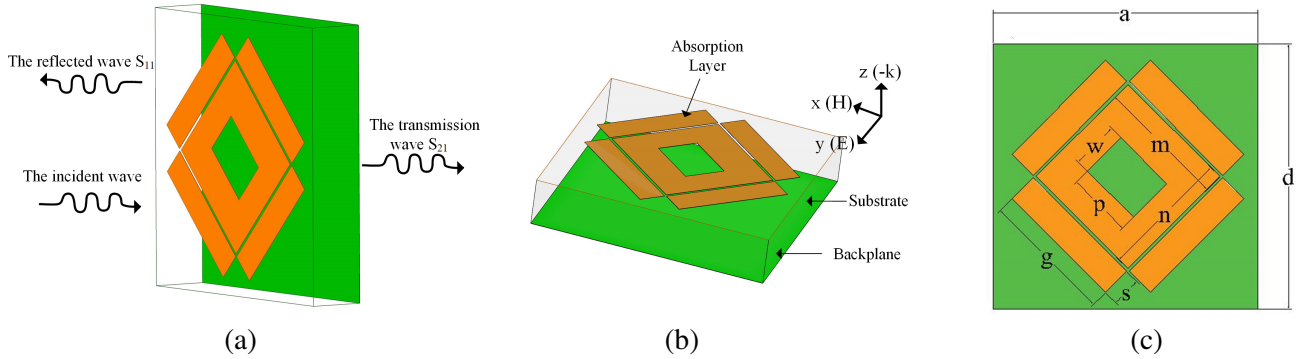

Figure 2. Electromagnetic wave propagation and unit structure diagram. (a) Schematic diagram of scattering parameters; (b) overall view of structure; (c) top view of structure.

The absorber structure in this paper has three layers: the resonant metal layer, dielectric layer, and metal's reflective backplane. Figure 2 shows the structure of the absorber unit designed in this paper. Figure 2(b) shows the three-dimensional diagram of the metamaterial unit structure. The dielectric layer is chosen from an FR-4 dissipative dielectric plate, whose relative dielectric constant is 4.5, and the loss angle tangent is 0.02. Both the resonant layer and reflective backplate use metallic copper with a thickness of 0.017 mm and conductivity of 5.8×10^7 S/m. The metal resonant layer unit structure with the metal square ring and four rectangular metal combinations is shown in Figure 2(c), where the metal square ring and four rectangular metal combinations. The equivalent inductance L and capacitance C of the resonant layer can be adjusted by changing the geometry and relative position of the metal square ring and four rectangular metals.

The thickness of the dielectric layer is 3.2 mm, and the dimensions of the metamaterial cell are 16 mm × 16 mm × 3.234 mm, $a = 16$ mm, $d = 16$ mm, $g = 8$ mm, $s = 1.8$ mm, $p = 3.925$ mm, $w = 2.85$ mm, $m = 7.85$ mm, $n = 7.85$ mm. Figure 5 shows the relationship between the reflection coefficient and absorbance with frequency when a plane wave is an incident vertically. The absorbance is greater than 90% of the frequency range of 8.06–18.46 GHz; the absolute bandwidth is 10.4 GHz; and the relative bandwidth reaches 76.9%, reaching the electromagnetic wave broadband absorption standard. The impedance matching curve of the absorber at this point is shown in Figure 6, which shows that the actual impedance of the absorber is basically the same as the ideal impedance within 8.06–18.46 GHz, thus achieving broadband microwave absorption.

The absorption curve shown in Figure 3 has two distinct absorption frequency bands with central frequency points of 10.95 GHz and 14.20 GHz, respectively. The absorption mechanism of the absorber can be explained based on the two resonant central frequency points of the metal resonance layer, such as the current distribution and field distribution.

The impedance matching curve of the electromagnetic metamaterial absorber shown in Figure 4 shows that the absorber meets the overall real impedance close to 377 Ω and the imaginary impedance close to 0 Ω in the range of 8–18 GHz. The impedance of the absorber is approximately equivalent

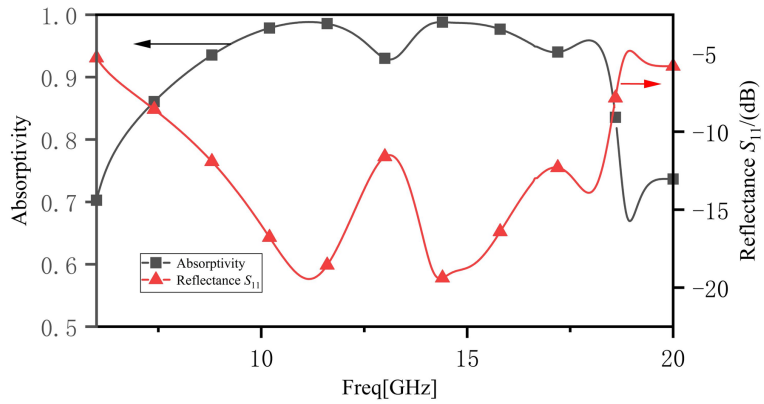

Figure 3. Variation curves of metamaterial reflection coefficient and absorption rate with frequency when plane wave is incident vertically.

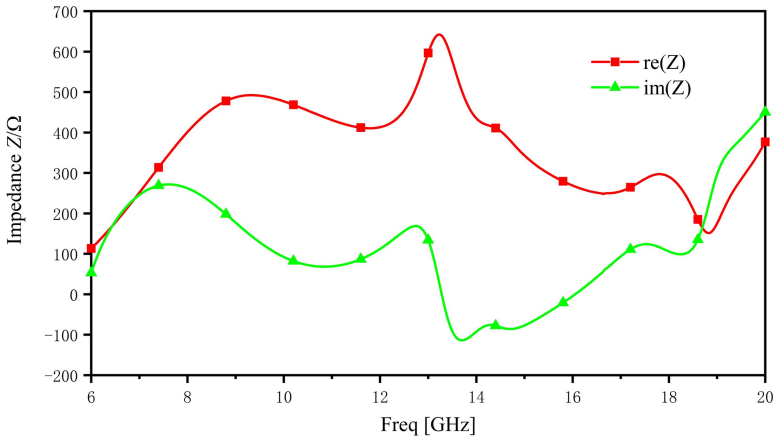

Figure 4. Impedance matching curve for electromagnetic metamaterial absorbers at vertical plane wave incidence.

to the free-space impedance, which improves the absorber's absorption rate by not refracting the electromagnetic waves when they are incident on the absorber.

Analyzing the absorption mechanism of this absorber, the absorption curve shown in Figure 3 has two distinct absorption frequency bands with central frequency points of 10.95 GHz and 14.20 GHz, respectively. The surface current J, surface electric field E, and body loss density distribution corresponding to the two central frequency points are given in Figure 5. As shown in Figures 5(a) and (b), under the influence of the incident electromagnetic wave, the free electrons in the metal resonant layer move in a fixed direction, forming an induced surface current, and the direction of the induced current is parallel to the direction of the applied electric field, resulting in ohmic loss, which consumes part of the incident electromagnetic wave energy. In addition, the positive charge moves in the direction of the applied electric field and gathers at the intersection of the upper side of the square ring and the upper two rectangular metals. In contrast, the negative charge moves against the direction of the electric field and gathers at the intersection of the lower side of the square ring. The lower two rectangular metals, i.e., the induced surface electric field, are formed between adjacent periodic cells, as shown in Figures 5(c) and (d). Due to the influence of the induced electric field, the metal resonant and dielectric layers will be polarized, and the electric dipoles in the resonant and dielectric layers will be arranged in the same direction as the electric field. The electric dipole will convert the electromagnetic wave energy into heat during the polarisation process, resulting in a body loss, as shown in Figures 5(e) and (f). Ultimately, the incident electromagnetic wave will be consumed in the form of both ohmic and dielectric losses.

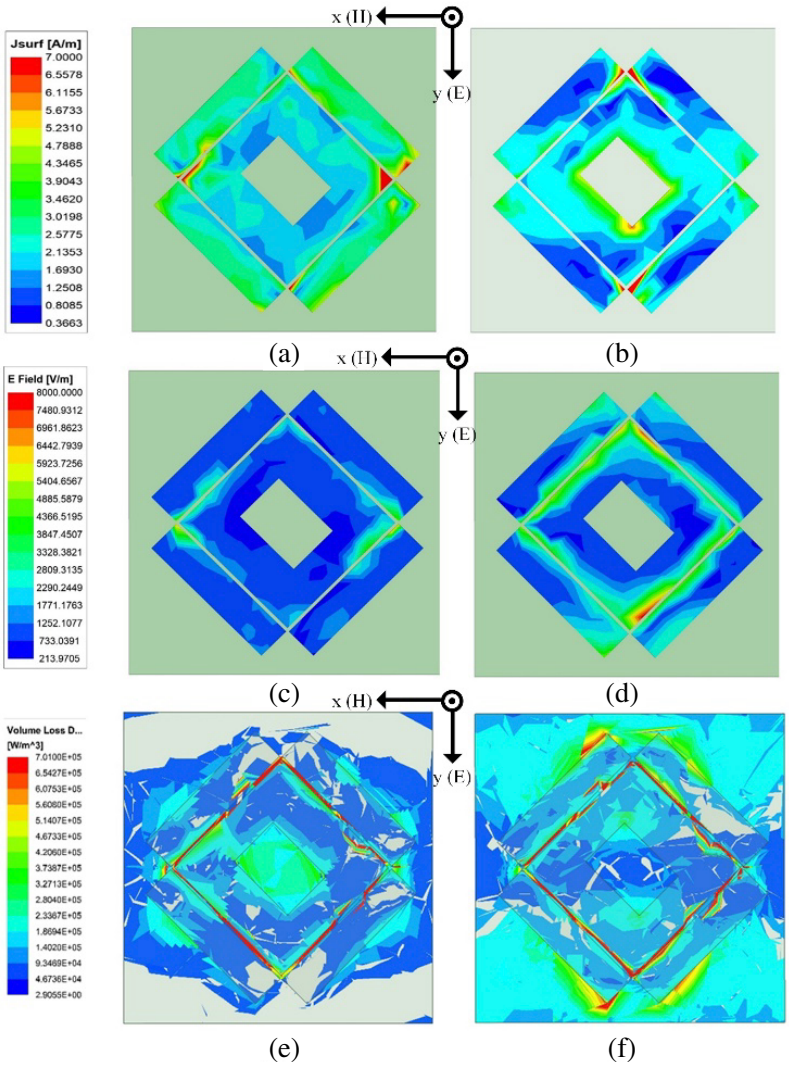

Figure 5. Losses of metamaterials when plane waves are incident vertically. (a) 10.95 GHz surface current amplitude; (b) 14.20 GHz surface current amplitude; (c) 10.95 GHz surface electric field amplitude; (d) 14.20 GHz surface electric field amplitude; (e) 10.95 GHz bulk loss density; (f) 14.20 GHz bulk loss density.

Since electromagnetic metamaterial absorbers are usually related to polarisation and angle of incidence, the angle of incidence-dependent absorption efficiency should be characterised. For transverse electric (TE) electromagnetic waves and transverse magnetic (TM) electromagnetic waves, the absorption characteristics of this absorber for electromagnetic waves incident obliquely at different angles are simulated. Figures 6 and 7 show the absorption curves of TE and TM electromagnetic waves incident obliquely at different angles into the electromagnetic metamaterial absorber. It can be observed that the absorption rate does not change significantly when the TE and TM waves are incident at an oblique angle into the electromagnetic metamaterial absorber, indicating that the absorber is not sensitive to the polarisation mode and incident angle.

4. EXPERIMENTS AND RESULTS

A corresponding suction device was fabricated to verify the feasibility of the proposed electromagnetic metamaterial-based suction device in this paper. The overall size of the structure is 160 mm × 160 mm

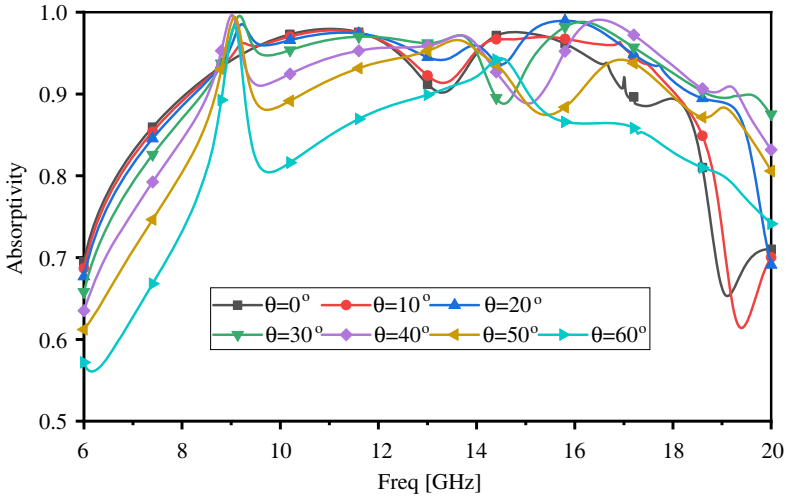

Figure 6. Absorption rate of oblique incident TE wave.

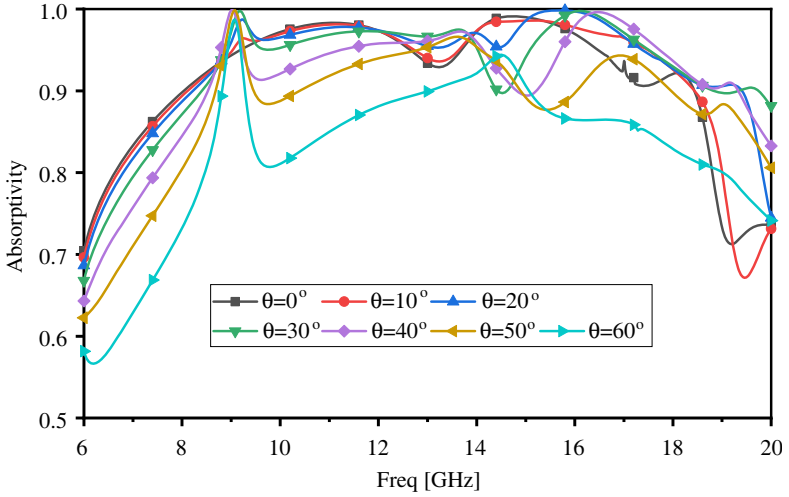

Figure 7. Absorption rate of oblique incident TM wave.

(10 × 10 cells), as shown in Figure 8. The metal resonant layer cells were etched onto an FR-4 dielectric substrate of 3.2 mm thickness by etching a printed circuit board. The absorbers were physically measured using the bow measurement method in a microwave darkroom. A vector network analyser was connected to two wide ridge horn antennas to measure the absorbance, as shown in Figure 9.

The simulated and measured results are shown in Figure 10, although the measured results show that the absorption rate of the absorber is greater than 90% in the frequency band of 8.04 GHz–18.64 GHz, which is basically consistent with the simulated results. However, the measured results deviate slightly from the simulated ones. The errors may be due to: (i) errors in the FR-4 dielectric substrate used in the sample and the simulated value; (ii) processing errors caused by the limitations of the processing technology and accuracy; (iii) scattering and bypassing effects at the edge of the absorber sample and scattering between the transmitting and receiving antennas.

Overall, the actual measured values are consistent with the simulation results, verifying the absorber's correct design and the practical application's feasibility.

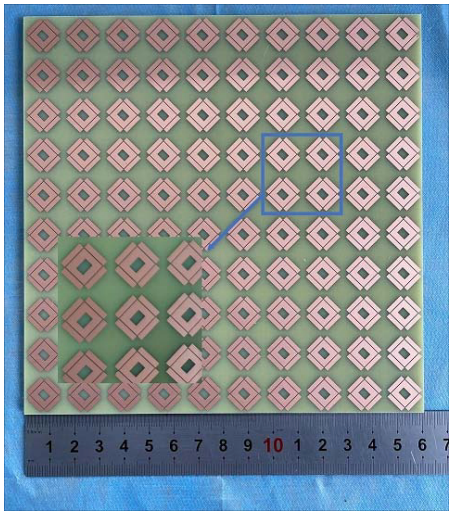

Figure 8. Real picture of electromagnetic metamaterial absorber.

Figure 9. Absorption rate of electromagnetic metamaterial absorber at different polarization angles.

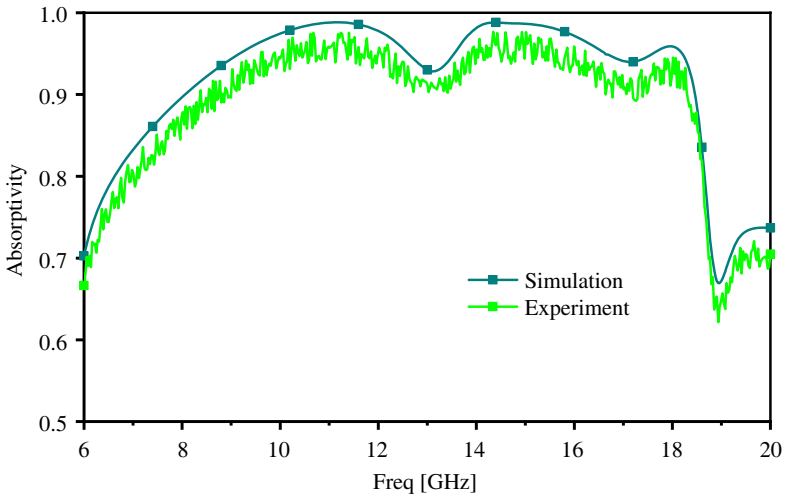

Figure 10. Comparison curve between simulation and test results of absorber absorption rate.

5. ANALYSIS AND DISCUSSION

The broadband electromagnetic metamaterial absorber has gradually become one of the performance criteria for measuring absorbers in recent years due to its wide absorption bandwidth, wide frequency coverage, and large application value. The absorption oscillator proposed in this paper is compared with an approximate resonance-type absorption oscillator, as shown in Table 1, where f_L and f_H indicate the lowest and highest frequency values of the absorption band where the absorption rate exceeds 90%, respectively. As seen from the table, the absorption bandwidth obtained varies with the resonant layer structure of the absorber. Compared with several absorbing structures mainly proposed in recent years, the broadband absorber in this paper has a simple structure, thin thickness, and better wide-angle absorption characteristics. It greatly extends its application range.

Table 1. Comparison of an approximate resonant structure absorber with the absorber proposed in this paper.

Reference	*Resonance structure*	*Bandwidth f_L-f_H (GHz)*	*Periodicity (λ_L)*
[19]	Second order cross typing element	4–8	0.013
[20]	Concave disc resonator and resistance film	1–7	0.0067
[21]	Double ring resonator	4.19/9.75	0.00695
[22]	Cross and its complementary structure	4.99–5.39	0.083
[23]	Split ring structure based on lumped elements	2.85–5.31	0.048
This work	Square metal ring with long straight wire	8.06–18.64	0.086

6. CONCLUSION

In this paper, an electromagnetic metamaterial-based broadband absorber is designed. Using the impedance matching theory, the impedance of the absorber in the frequency band of 8.06 GHz–18.46 GHz is approximated to the free space impedance. The absorber consistently achieves more than 90% efficient absorption of incident electromagnetic waves in the 8.06 GHz–18.46 GHz band, with a total bandwidth of 10.40 GHz, and a broadband absorption effect. In TE and TM modes, the absorption rate of this absorber structure remains almost above 90% when the angle of oblique incidence of the electromagnetic wave into the absorber reaches 50°. When the polarisation angle of the electromagnetic wave is less than or equal to 50°, the simulation shows that the absorption rate of the structure is still greater than 90%, indicating that it has polarisation-insensitive absorption characteristics. The broadband absorber based on electromagnetic metamaterials has the characteristics of a wide absorption band, high absorption rate, and the absorption performance of insensitivity to the incident angle. The study provides an idea for the design and development of new broadband absorbers.

REFERENCES

1. Veselago, V. G., "Electrodynamics of substances with simultaneously negative ε and μ," *Usp. Fiz. Nauk*, Vol. 92, No. 7, 517–526, 1967.
2. Feng, Y. J., B. Zhu, P. H. Xu, et al., "Application of electromagnetic metamaterial in microwave absorbing materials," *Progress of Materials in China*, Vol. 32, No. 8, 473–479, 2013.
3. Zhang, L., S. Liu, and T. J. Cui, "Theory and applications of electromagnetically encoded metamaterials," *China Optical*, Vol. 10, No. 1, 1–12, 2017.
4. Wang, G. D., "Design of electromagnetic metamaterial and study of its absorbing properties," *Huazhong University of Science and Technology*, 2014.
5. Jain, P., A. K. Singh, J. K. Pandey, et al., "Ultra-thin metamaterial perfect absorbers for single-/dual-/multi-band microwave applications," *IET Microwaves, Antennas & Propagation*, Vol. 14, No. 5, 390–396, 2020.
6. Jain, P., A. K. Singh, J. K. Pandey, et al., "An ultrathin compact polarization-sensitive triple-band microwave metamaterial absorber," *Journal of Electronic Materials*, Vol. 50, No. 3, 1506–1513, 2021.
7. Jain, P., K. Prakash, G. M. Khanal, et al., "Quad-band polarization sensitive terahertz metamaterial absorber using Gemini-shaped structure," *Results in Optics*, Vol. 8, 100254, 2022.
8. Zhou, J., E. N. Economon, T. Koschny, et al., "Unifying approach to left-handed material design," *Optics Letters*, Vol. 31, No. 24, 3620–3622, 2006.
9. Bui, S. T., Y. J. Yoo, K. W. Kim, et al., "Small-size metamaterial perfect absorber operating at low frequency," *Advances in Natural Sciences: Nanoscience and Nanotechnology*, Vol. 5, No. 4, 045008, 2014.

10. Khuyen, B. X., B. S. Tung, Y. J. Yoo, et al., "Miniaturization for ultrathin metamaterial perfect absorber in the VHF band," *Scientific Reports*, Vol. 7, No. 1, 1–7, 2017.
11. Zuo, W., Y. Yang, X. He, et al., "A miniaturized metamaterial absorber for ultrahigh-frequency RFID system," *IEEE Antennas and Wireless Propagation Letters*, Vol. 16, 329–332, 2016.
12. Li, H., L. H. Yuan, B. Zhou, et al., "Ultrathin multiband gigahertz metamaterial absorbers," *Journal of Applied Physics*, Vol. 110, No. 1, 014909, 2011.
13. Yoo, Y. J., H. Y. Zheng, Y. J. Kim, et al., "Flexible and elastic metamaterial absorber for low frequency, based on small-size unit cell," *Applied Physics Letters*, Vol. 105, No. 4, 041902, 2014.
14. Ghosh, S., S. Bhattacharyya, Y. Kaiprath, et al., "Triple-band polarization-independent metamaterial absorber using destructive interference," *2015 European Microwave Conference (EuMC)*, 335–338, IEEE, 2015.
15. Bhattacharyya, S., S. Ghosh, and K. V. Srivastava, "An ultra-thin polarization independent metamaterial absorber for triple band applications," *2013 IEEE Applied Electromagnetics Conference (AEMC)*, 1–2, IEEE, 2013.
16. Shen, X., T. J. Cui, J. Zhao, et al., "Polarization-independent wide-angle triple-band metamaterial absorber," *Optics Express*, Vol. 19, No. 10, 9401–9407, 2011.
17. Hu, D., J. Cao, W. Li, et al., "Optically transparent broadband microwave absorption metamaterial by standing-up closed-ring resonators," *Advanced Optical Materials*, Vol. 5, No. 13, 1700109, 2017.
18. Amiri, M., F. Tofigh, N. Shariati, et al., "Miniature tri-wideband Sierpinski-Minkowski fractals metamaterial perfect absorber," *IET Microwaves, Antennas & Propagation*, Vol. 13, No. 7, 991–996, 2019.
19. Huang, D., F. Kang, C. Dong, et al., "A second-order cross fractal meta-material structure used in low-frequency microwave absorbing materials," *Applied Physics A*, Vol. 115, No. 2, 627–635, 2014.
20. Nie, Y., Y. Z. Cheng, and R. Z. Gong, "A low-frequency wideband metamaterial absorber based on a cave-disk resonator and resistive film," *Chinese Physics B*, Vol. 22, No. 4, 044102, 2013.
21. Singh, A. K., M. P. Abegaonkar, and S. K. Koul, "Dual-and triple-band polarization insensitive ultrathin conformal metamaterial absorbers with wide angular stability," *IEEE Transactions on Electromagnetic Compatibility*, Vol. 61, No. 3, 878–886, 2018.
22. Wang, Y., L. Wang, J. Song, et al., "Experimental analysis and comparison between cross-shaped metamaterial absorber and its complementary structure," *Microwave and Optical Technology Letters*, Vol. 61, No. 4, 930–936, 2019.
23. Yuan, W. and Y. Cheng, "Low-frequency and broadband metamaterial absorber based on lumped elements: Design, characterization and experiment," *Applied Physics A*, Vol. 117, No. 4, 1915–1921, 2014.